

## A Pan-STARRS1 Search for Planet Nine

MICHAEL E. BROWN <sup>1</sup>, MATTHEW J. HOLMAN <sup>2</sup> AND KONSTANTIN BATYGIN <sup>3</sup>

<sup>1</sup>*Division of Geological and Planetary Sciences  
California Institute of Technology  
Pasadena, CA 9125, USA*

<sup>2</sup>*Center for Astrophysics  
Harvard & Smithsonian  
60 Garden Street, Cambridge, MA 02138, USA*

<sup>3</sup>*Division of Geological and Planetary Sciences  
California Institute of Technology  
Pasadena, CA 9125, USA*

### ABSTRACT

We present a search for Planet Nine using the second data release of the Pan-STARRS1 survey. We rule out the existence of a Planet Nine with the characteristics of that predicted in Brown & Batygin (2021) to a 50% completion depth of  $V = 21.5$ . This survey, along with previous analyses of the Zwicky Transient Facility (ZTF) and Dark Energy Survey (DES) data, rules out 78% of the Brown & Batygin parameter space. Much of the remaining parameter space is at  $V > 21$  in regions near and in the area where the northern galactic plane crosses the ecliptic.

### 1. INTRODUCTION

Speculation about the existence of planets beyond the orbit of Neptune began almost as soon as the announcement of the discovery of Neptune itself (Babinet 1848) and has continued to the present day. While Standish (1993) demonstrated that no evidence exists in the planetary ephemerides for any significant perturber, the concurrent discovery of the large population of small bodies in the Kuiper belt beyond Neptune led to renewed scrutiny of dynamical signatures of perturbation in this population. The first concrete hint of the need for an external perturber – at least at some point in solar system history – came from the discovery of Sedna,

with a perihelion at 76 AU, well beyond where it could have been perturbed by the known planets (Brown et al. 2004). As more objects with the extreme semimajor axis of Sedna were discovered, they were suggested to be anomalously clustered around an argument of perihelion of zero, though the physical mechanism for the apparent clustering was unclear (Trujillo & Shepard 2014). Subsequent analysis showed that the apparent clustering in argument of perihelion is actually a consequence of simultaneous clustering in longitude of perihelion and in pole position, a phenomenon that can be naturally explained by the presence of a massive planet on a distant, eccentric, and inclined orbit (Batygin & Brown 2016a). The prediction of the existence of this planet has been called the Planet Nine hypothesis. Planet Nine is now seen to be capable of accounting for a range of addi-

tional otherwise unexplained phenomena in the solar system, including the existence of highly-inclined Kuiper belt objects and the existence of retrograde Centaurs (Batygin & Brown 2016b).

Since the prediction of the existence of this planet, discussions of alternative explanations have included suggestions that it is instead a primordial black hole (Scholtz & Unwin 2020), that the observed effects are caused by the presence of a distant unseen ring of material (Madigan & McCourt 2016; Sefilian & Touma 2019), or that the planet is instead a collection of condensed dark matter (Sivaram et al. 2016), though a planet remains a far simpler explanation than these exotic possibilities. Suggestions that observational bias might be responsible for the observed clustering effects have been made from analysis of limited data sets (Shankman et al. 2017; Napier et al. 2021), but analysis of the largest data sets has repeatedly found the probability of such bias small (Brown & Batygin 2019, 2021). While the existence of Planet Nine remains the most satisfactory explanation for a range of phenomena, true detection of the planet will be required to firmly discount these or other alternatives.

The Planet Nine hypothesis makes distinct predictions about the properties of the planet and its orbit, based on the currently observed distant eccentric Kuiper belt population and on an assumed source population for these bodies. Under the assumption that the currently observed distant eccentric population is sourced from an initial extended disk (rather than, i.e. from the inner Oort cloud, Batygin & Brown (2021); Nesvorný et al. (2023)), Brown & Batygin (2021, hereafter BB21) use a suite of numerical models corrected for observational bias to construct statistical distributions of the mass and orbital elements of the hypothetical Planet Nine consistent with the observed clustering. All elements are well constrained except for the mean anomaly; the current observations show

only the orbit of Planet Nine, not the position within the orbit. To aid in the search for Planet Nine and to better understand search limits for different surveys, Brown & Batygin (2022, hereafter BB22) construct a synthetic population by sampling from the posterior of the BB21 mass and orbital element distributions. This synthetic population can be injected into any data set to give a statistical representation of Planet Nine parameter space and determine which parts of parameter space a survey can rule out.

The first wide-field search for Planet Nine examined three years of the Zwicky Transient Facilities (ZTF) archives (BB22). This search covered most of the predicted path of Planet Nine (with the exception of regions below  $-25$  in declination and in the densest regions near the galactic center) and concluded that a Planet Nine candidate with the predicted parameters was not detectable in the archive. Though typical ZTF images reach a depth of only  $r \sim 20.5$ , injection of the synthetic population into the ZTF catalog showed that ZTF was sensitive to 56% of the predicted parameter space of Planet Nine.

The Dark Energy Survey (DES) covered only a modest fraction of the predicted orbital path of Planet Nine, but the entire survey region was surveyed for moving objects with distances from 30 - 2000 AU (Bernardinelli et al. 2022). No Planet Nine or other distant object candidates were found. Belyakov et al. (2022) used the previously developed synthetic population to show that the DES ruled out 10.2% of the predicted phase space of Planet Nine, of which 5.0% had not previously been ruled out by ZTF. Between the ZTF and DES survey 61.2% of the predicted Planet Nine phase space has been ruled out.

Here, we extend the search for Planet Nine to the Pan-STARRS1 DR2 (PS1) data base. PS1 observed a similar amount of sky as ZTF, but with deeper – though less frequent – coverage. For much of the sky, PS1 should extend the

magnitude limit of the search for Planet Nine by approximately a magnitude.

## 2. THE PAN-STARRS1 DATA

The Pan-STARRS1 survey covered the approximately  $3\pi$  steradians of the sky north of a declination of  $-30^\circ$ . Each area in the sky was covered approximately 12 times from 2009 to 2015 in each of 5 broadband filters (*grizy* reaching a single epoch depth of approximately 22.0, 21.8, 21.5, 20.9, 19.7, respectively). If Planet Nine was detected by PS1, it would appear as a single night transient in each detection. To search for Planet Nine, we will search for collections of single night transients which appear at locations consistent with a Keplerian motion moving on an orbit within the range of parameters predicted by [Brown & Batygin \(2021\)](#).

Directly querying the PS1 catalog for single night transients is not possible, so to construct our list of single night transients, we begin by using the PS1 CasJobs SQL server<sup>1</sup> to download every detection of every cataloged object for which there were fewer than 12 detections, with at least one of those detections in the *g*, *r*, or *i* bands which would be most sensitive to a solar-colored Planet Nine. Downloading these data in small batches required several months of continuous querying of the server. Many of these collections of up to 12 detections will be real stationary astrophysical sources which appear at the same location on multiple nights. Thus, after downloading, we discarded any object for which the detections of a cataloged object occurred on more than a single date. Over the Planet Nine search region – defined as the declination range over which 99% of the Planet Nine synthetic population occurs – we find 1.26 billion single night objects, most of which consist of a single detection in a night, but a small

number consisting of between 2 and 11 detections at a single location in one night.

The vast majority of single night transients in PS1 at the faint end are not real astrophysical sources, but rather arise from systematic noise ([Chambers et al. 2016](#)). Our goal is to find any set of transients that appear to follow a Keplerian orbit consistent with that predicted for Planet Nine over the five year period of the data. Finding such a set in the background of a billion bad detections is formidable problem. We thus explore ways to remove at least some of these bad detections. Any method which removes bad detections has the possibility of removing real detections also, thus we develop a method of calibration to take this possibility into account in the next Section.

To better understand the characteristics of real single night transients, we extract any detections within the data set of the first 501090 numbered asteroids by selecting every detection within 2 arcseconds and 2 magnitudes of an asteroid’s predicted position and brightness at each moment of observation. We have high confidence that those detections are nearly all real, as chance alignments on the scale of 2 arcsecs on individual PS1 exposures are rare, despite the abundance of spurious detections. This sample probes the full magnitude range of potential PS1 detections including the faintest end where the asteroids detected are those which were initially discovered at closer distances and were thus brighter but are now more distant and can have brightness at and well beyond the PS1 magnitude limit.

We examine these 6.21 million asteroid detections and find that we can use two parameters extracted from the PS1 database, PSFCHI2 and PSFQF (measures of the fit of the detection to the PSF and of the total coverage of the detection to the PSF), to help eliminate some of the most likely false positives. We make a simple cut and include only detections

<sup>1</sup> <http://mastweb.stsci.edu/ps1casjobs/>

with PSFQF greater than 0.99 and, for objects with a magnitude less than 16, PSFCHI2 between 0 and 8, and for fainter objects, PSFCHI2 between 0 and 1.6. We also reject all objects with a reported magnitude fainter than 22.5 as this magnitude is both beyond the stated depth of PS1 and our asteroid detections quickly drop before this magnitude. These simple cuts reduce the number of objects detected as single night transients to 772 million.

Significant spatial structure still exists in the locations of the remaining objects. A plot of the position of each object on the imaging array shows that each of the 60 individual detectors has distinct regions with greatly increased numbers of detected objects. We create individual masks for each of the 60 detectors by hand, and discard all objects within these masked regions. This masking reduces the number of objects under consideration to 428 million.

Another source for large number of clustered objects is scattered light from bright stars. We use the ATLAS REFCAT2 star catalog (Tonry et al. 2018) to examine the positions of all bright stars in the data. Stars fainter than about  $r \sim 13$  have limited issues with scattered light, but brighter stars are surrounded by clusters of objects. The radius of these clusters increases with the brightness of the star. We empirically define a bright star exclusion radius,  $r_e$ , based on  $m_r$ , the  $r$  magnitude in REFCAT2, as

$$r_e = 50 + 0.08(13 - m_r)^4$$

where  $r_e$  is in arcseconds. After excluding these objects, 314 million objects remain.

Even with detector masking and regions around bright stars excluded, clusters of objects can sometimes be found associated with individual image frames. We find that these can be effectively identified by using a clustering algorithm. Specifically, we remove all collections of 5 or more objects occurring within 40 arcseconds of each other. This final cut reduces our data set to 244 million objects.

We have reduced our original data set from 1.2 billion to 244 million objects, a decrease of 80%. While searching for Planet Nine through this large data set remains a formidable task, we could find no additional filters that appeared to safely further reduce the data set. Any one of these cuts in the data has the possibility of removing real detections of Planet Nine. Our calibration method must by necessity take this possibility into account.

### 3. CALIBRATION

The footprints and depths of individual PS1 pointings are not easily available, thus we use the method developed in BB22 to self-calibrate the data set. In short, we use the asteroids identified above as probes of both the coverage and depth of PS1 on individual nights.

We use the JPL Horizons system<sup>2</sup> to calculate the positions and magnitudes of the first 501090 numbered asteroids for each night of the 5 year PS1 survey. We interpolate the positions to the time of each image taken during a night and keep a log of which asteroids are and which are not detected each night and of what their predicted  $V$  magnitude for that night was. We record this information in  $\sim 1.8$  square degrees patches of the sky using an NSIDE=32 HEALPix grid<sup>3</sup>. A typical HEALPix cell near the ecliptic has hundreds of asteroid detections per night and even at the maximum distance from the ecliptic searched, many asteroids are available. From this dataset we now have a nightly record of asteroid detections and non-detections as a function of predicted magnitude within each HEALPix footprint that we can use to calibrate the detectability of Planet Nine on any night at any position. Note that we exclusively work in predicted  $V$  band magnitude, ignoring the actual filter used for each obser-

<sup>2</sup> [ssd.jpl.nasa.gov](http://ssd.jpl.nasa.gov)

<sup>3</sup> <https://healpix.jpl.nasa.gov>

vation. This method is equivalent to assuming that Planet Nine has the same color as the average asteroid. The effects of other color assumptions are generally small and discussed in [Belyakov et al. \(2022\)](#). BB22 examined the use of predicted asteroids magnitudes as calibrators and found that there were no systematic offsets between the asteroid predictions and measured brightnesses, and that the RMS deviation between predictions and measurements is 0.2 magnitudes. We thus conclude that our self-calibration with asteroids is accurate to approximately this level. Note that these asteroid extractions are performed after all of the data filtering discussed above, thus they correctly account for any real detections that would have been inadvertently removed in the filtering.

We next make use of the Planet Nine reference population of BB22. BB22 created a sample of 100000 potential Planets Nine drawn from the statistical model of BB21 for the orbital parameters and mass of Planet Nine. They assumed a simple mass-diameter relationship of  $r_9 = (m_9/3)R_{\text{earth}}$ , where  $m_9$  is in Earth masses and  $R_{\text{earth}}$  is the mass of the Earth, based on fits to planets in this radius and mass range ([Wu & Lithwick 2013](#)), and assume albedos from half that of Neptune, 0.2, to a value predicted by a model in which all absorbers are condensed out of the atmosphere ([Fortney et al. 2016](#)), 0.75. Each Planet Nine was assigned a mean anomaly on a reference date of 1 June 2018, so their position, distance from the sun, and brightness can be predicted for any night. For each member of this reference population, we calculate the position of the the body for each night of the PS1 survey, determine the apparent magnitude of the body (ignoring the small contribution from phase effects), and calculate the HEALPix grid point in which it would appear. We then use the record of asteroids detected and not detected on that night in that grid point to determine the probability that Planet Nine with its predicted

magnitude would have been detected on that night. We then randomly select a number between 0 and 1 and, if that number is lower than the detection probability, we record a detection of a member of the reference population at that position – with an astrometric offset randomly applied based on the reported uncertainties of asteroids of the same magnitude – and magnitude. Note that we do not explicitly consider whether Planet Nine would be detected in a specific exposure on a night, but just whether it would have been detected on any exposure that night and thus result in a transient object in our PS1 database. We embed these reference population detections into our PS1 data and use them for the ultimate calibration of the survey.

The PS1 survey is extremely sensitive to the predicted range of potential Planets Nine. Of the 100000 members of the reference population, 88736 would be detected at least once, with 69082 detected nine times or more. The variable night-to-night detection limit at the faint end is ultimately responsible for the stochastic nature of detections of the faintest members of the population (as would be the case for detection of the real Planet Nine at this magnitude).

#### 4. ORBIT LINKING

Examining 244 million detections of transient objects made over a 5 year period to find any set of objects consistent with Keplerian motion is a computational intensive task. A variation of the algorithm developed by [Holman et al. \(2018\)](#) and implemented in BB22 greatly speeds this process. The process, described in detail in BB22, begins with the simplifying realization that, when viewed from the sun, Keplerian orbits travel in simple great circles across the sky. At the large distance of Planet Nine, the motions are essentially a constant velocity over long time spans.

To determine if a transient object is part of a collection of objects consistent with a Keplerian

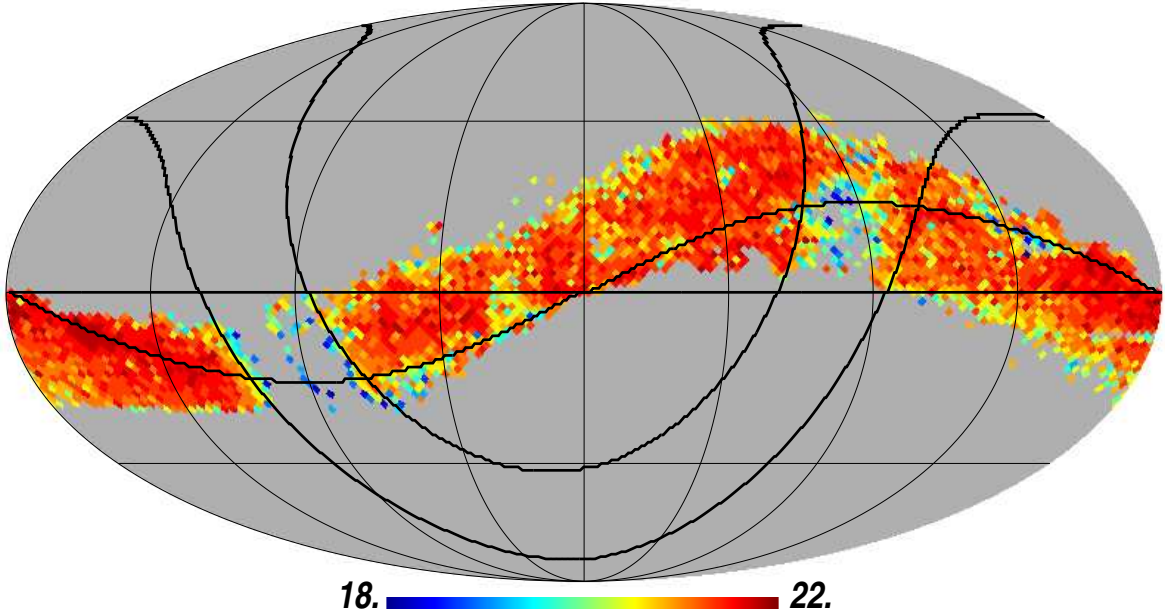


**Figure 1.** The  $V$ -band magnitude at which there is a 95% or higher probability that a moving object would be detected 9 or more times in the portion of the PS1 data that intersects the predicted locations of P9. The data are shown in a Mollweide equal area projection in equatorial coordinates. Right ascension of 360 is on the left with 180 in the middle and 0 on the right. The ecliptic is indicated by a line, as well as galactic latitudes of  $\pm 15^\circ$ .

orbit, the algorithm takes the object, assumes a range of heliocentric distances for this object, and transforms all other detected transient objects from their observed geocentric RA and dec to their heliocentric longitude and latitude as if they were at the assumed heliocentric distance and observed from the sun. Any real detection of a Solar System body on a distant Keplerian orbit will now appear as a collection of transient objects on a great circle at different dates, separated by a constant angular speed between the detections. To search for such a collection, angular velocity vectors are calculated from the initial transient object to every other transient

object in the heliocentric system. A real detection will now appear as a cluster of objects with similar angular velocity vectors. A small spread in angular velocity vectors occurs even for a real detection owing to the discrepancy between the assumed and true distance of the object, but can also occur because the collection of objects is spurious and due to chance and does not precisely conform to a Keplerian orbit. Thus for every cluster of objects (with a cluster size larger than a given number threshold, discussed below), the cluster of objects (plus the original object) is fit to a full Keplerian orbit with the algorithm of [Bernstein & Khushalani](#)

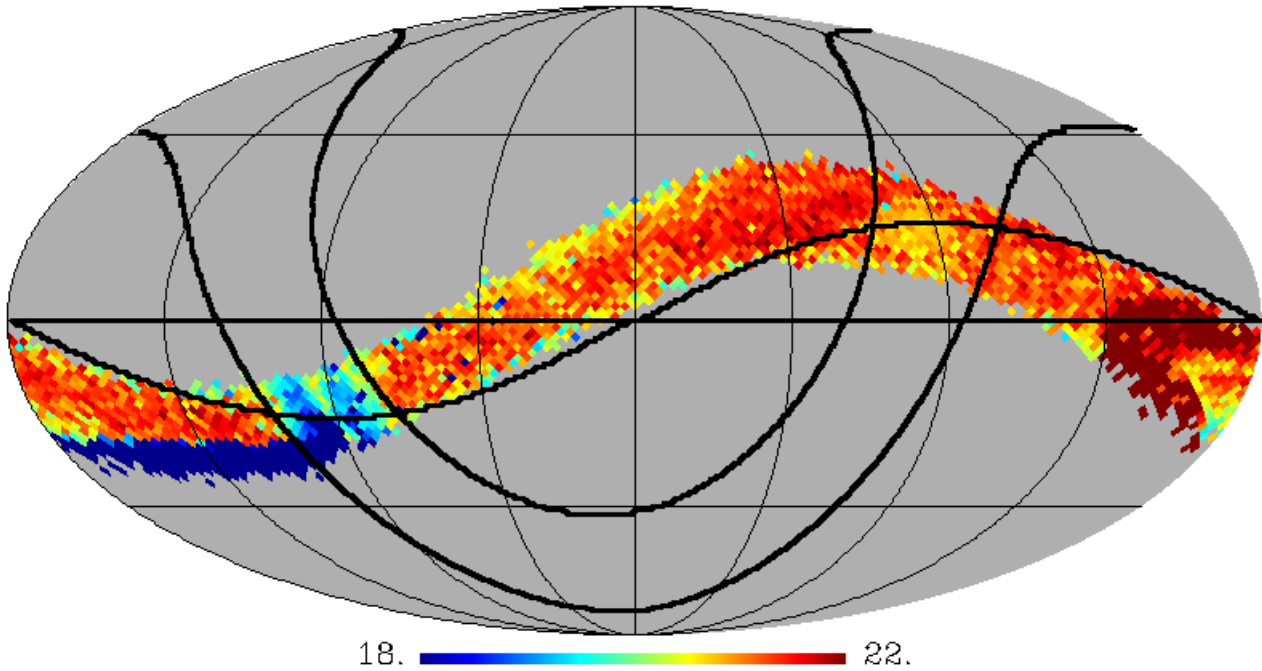


**Figure 2.** The combined  $V$ -band magnitude limits of the ZTF, DES, and PS1 surveys for Planet Nine, reconstructed from detections of the synthetic reference population. The geometry is the same as Fig. 1. Note that the sky area is smaller than in Fig. 1 because we require a minimum of 4 members of the reference population to be present to estimate a limit. The deep DES survey on the far right has magnitude limits that extend as far as 24. The areas in dark blue remain unsurveyed.

(2000), and the astrometric residuals are determined. If the residuals are below a given threshold, the set of objects is retained as a candidate for a detection of a real object with Keplerian motion.

For the PS1 data, we implement this algorithm on the latitudinal swath of sky that contains 99% of the reference population at each longitude. We further restrict the analysis to motions and distances consistent with this reference population. Distant objects which exist but do not fit the Planet Nine hypothesis will therefore not be found in this analysis. Faster linking algorithms or increased processing power will be required before such a larger analysis is possible.

Several choices must be made for the analysis algorithm, including the spacing of assumed

heliocentric distances, the size of an angular velocity box to be used to identify clusters of potentially linked objects, the threshold for the minimum number of objects to consider a link, and the astrometric threshold to retain the linkage as a true candidate. These choices involve a complex set of trade offs. For example, a wider spacing of assumed heliocentric distances leads to fewer geometric transforms but also to the need to use a larger box in angular velocity for identifying clusters, as the discrepancy between the true and assumed distance causes the spread of angular velocities to increase. The larger angular velocity box causes more spurious clusters which must be checked with the full Keplerian fitting, drastically slowing the search. The most efficient trade off is a function of the number density of detections on the sky. Similarly, the

threshold for the number of objects required to be within a cluster before full Keplerian orbit fitting is a critical parameter. Requiring a large number of objects to be clustered before considering the cluster for Keplerian fitting greatly speeds the processing speed at the expense of potentially missing the real Planet Nine if it is detected a smaller number of times. A lower threshold, in contrast, is computationally intensive and also leads to larger numbers of false positive linkages.

In all cases we choose these parameters in the same manner as they were chosen in BB22, by simulating different spacing for our assumed distances and different sizes for our angular velocity cluster box sizes in an attempt to minimize the processing time. While BB22 recalculated parameters at each location on the sky, here we simplify the analysis and use a single angular velocity cluster box width of 0.052 arcseconds  $\text{day}^{-1}$  in longitude and 0.026 arcseconds  $\text{day}^{-1}$  in latitude along with a constant spacing of our assumed distances in inverse heliocentric distance of  $\Delta(1/r) = 10^{-5} \text{ AU}^{-1}$ . We empirically find that these parameters come close to optimizing processing time while, as will be demonstrated below, also finding all possible linkages.

The final parameter to be selected is the minimum number of transient detections to be required to be considered a linked Keplerian orbit. In BB22 we required 7 detections over a 3 year period. The PS1 data has a significantly higher number density of (mostly spurious) objects on the sky, such that if we require only 7 detections we are overwhelmed with false linkages. We find that requiring 9 detections both improves the processing speed and brings the number of false positives to an acceptably low number.

With these parameters in place we can now visualize approximate limiting magnitudes for the possible detection of P9 in the PS1 survey. We use our asteroid database to calculate the mag-

nitude at which an object would be detected on 9 or more distinct dates in a HEALPix grid cell 95% of the time (Fig. 1). Assuming that our processing can efficiently link all such objects, the median magnitude limit for the detection of Planet Nine for a region outside of the galactic plane is  $V = 21.0$ . The northern galactic plane region has some area of coverage but has considerably worse limits, while the southern galactic plane region has almost no usable data.

## 5. RESULTS

The processing of the data was performed in  $3^\circ \times 3^\circ$  blocks across the sky. Enough overlap was included among the blocks to account for the fastest potential motion of P9 across the 5 year period of the data. Even with approximately 50 blocks running in parallel the full data set required several months of continuous processing time.

The catalog of simulated reference population detections was included in the processing, which had no knowledge whether the detection was from the real PS1 data or an artificially injected member of the reference population. Of the 69082 members of the reference population which had 9 or more detections, 68550 are correctly linked, for a success rate of 99.2%. We consider this a strong demonstration that, if a Planet Nine candidate consistent with the predicted parameters of BB21 existed in the PS1 data set and was detected 9 times or more, it would be efficiently discovered by our algorithm.

In the full dataset, 909 additional linkages are made. Each one of them is a chance linkage between multiple members of the reference population and a small number of fortuitously placed real PS1 detections (note that the algorithm allows multiple linkages between objects, so in each case the true linkage of the objects belonging to the reference population is still correctly made).

We conclude that no object with the predicted characteristics of P9 was detected nine or more



times in the PS1 data set. The magnitude limits shown in Fig. 1 provide a good approximation to the search limit, with the caveat that the search is only sensitive to objects with orbital characteristics similar to those predicted by BB21.

The reference population provides an effective method for combining the limits from the PS1 data with those already achieved by ZTF and DES. Of the 69802 members of the reference population detected, 17054 were unique to PS1. The total fraction of the reference population that has been ruled out by the combination of ZTF, DES, and PS1 is 78%. In Figure 2 we show an approximation of the full magnitude limit of the three combined surveys by examining each HEALPix grid point that contains 4 or more members of the reference population and setting the limit equal to the faintest object detected brighter than the brightest non-detection. When all objects in the grid point are detected we show the magnitude of the faintest object. Each of the surveys has regions of unique contribution. PS1 uniquely detects 17% of the reference population, mostly at high galactic latitudes at depths fainter than ZTF. ZTF uniquely detects 6%, predominantly in the northern galactic plane where PS1 coverage is poor. And DES uniquely detects 3% of the population at magnitudes fainter than PS1 covers. The remaining 52% of the detected population is detected by two or more surveys, most often ZTF+PS1 for the brighter objects at high galactic latitudes.

As is apparent, the combined surveys have a step-wise efficiency with magnitude (Fig. 3). The combined survey is about 94% efficient for objects brighter than  $V = 20.5$ , falling to a 50% efficient at  $V = 21.5$ . A large tail of detectable objects as faint as  $V = 23.5$ , exclusively from the DES observations, extends at  $\sim 20\%$  efficiency. Many of the missing bright objects are in the unobserved low declination regions

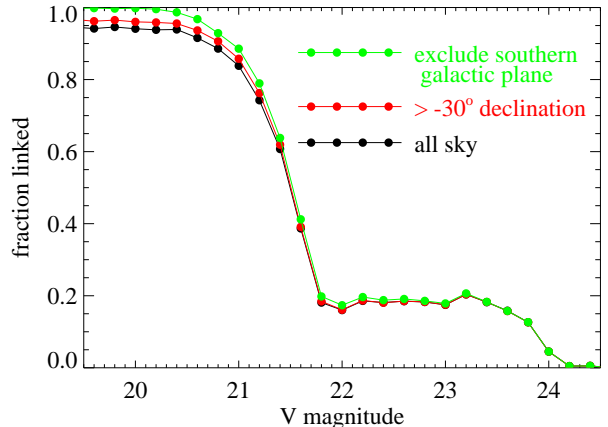


**Figure 3.** The fraction of the BB22 Planet Nine reference population that would have been detected by the ZTF, DES, and PS1 surveys, as a function of  $V$ -band magnitude. The combined surveys are extremely efficient for objects fainter than  $V \sim 21$  and reach 50% efficiency at  $V = 21.5$ , with a large tail of fainter detections from the deep but narrow DES survey.

or the poorly observed southern galactic plane. If these regions are excluded, the bright object efficiency increases to 97% and 99.7%, respectively. There is reason to believe that P9 would not be found at these locations: a full fit of planetary ephemerides and search for gravitational perturbations due to P9 suggests that a P9 near perihelion – as these southern hemisphere positions are – would have already been detected (Fienga et al. 2020). How best to combine these constraints with those derived here remains uncertain, however.

## 6. DISCUSSION

The combination of the ZTF, DES, and PS1 surveys rules out 78% of the BB22 P9 reference population. The sky positions of the remaining members of the Reference Population are shown in Figure 4. Using the members of the Reference Population yet to be ruled out, we update our predictions for P9 parameters. We report the median with the 15.8 and 84.1 percentile values as the uncertainties. Our

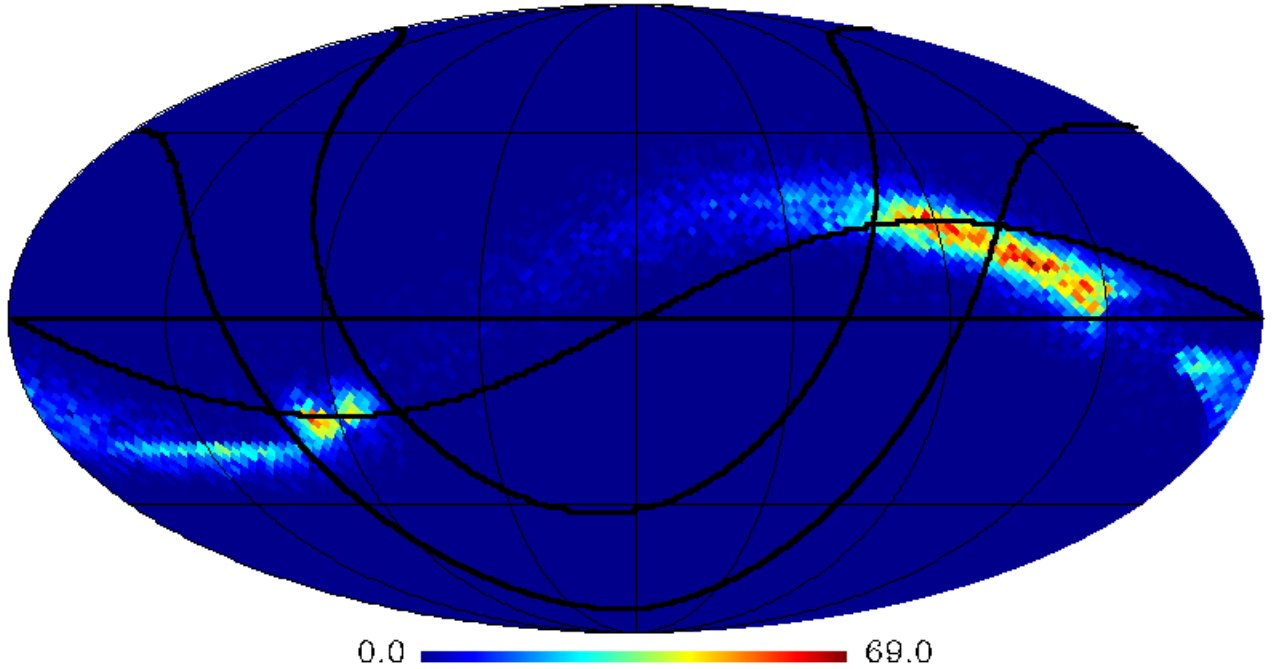


**Figure 4.** The probability density function of on-sky location of the BB22 Planet Nine reference population that would remain undetected after the ZTF, DES, and PS1 surveys. The geometry is the same as Figure 1.

newly updated estimates include a semimajor axis of  $500_{-120}^{+170}$  AU, a mass of  $6.6_{-1.7}^{+2.6} M_{\oplus}$ , an aphelion distance of  $630_{-170}^{+290}$  AU, a current distance of  $550_{-180}^{+250}$  AU, and a V magnitude of  $22.0_{-1.4}^{+1.1}$ . The other predicted parameters remain generally unchanged. All parameters and distributions of the Planet Nine reference population, including flags for whether the objects would have been found by ZTF, by DES, or by PS1, can be found permanently archived at <https://data.caltech.edu/records/8fjad-x7y61>

The remaining areas of P9 parameter space that remain unexplored, shown in Figure 4, include a large swath near the northern galactic plane where P9 is near aphelion and thus would be fainter than the current limits and a smaller region in the part of the southern galactic plane that remains poorly covered as well as a strip below a declination of  $-30^{\circ}$ . Much of this remaining parameter space will be covered by

the upcoming Vera Rubin Observatory survey, which will be sensitive to all but the faintest and most northern predicted positions.

While a large majority of the phase space for Planet Nine predicted by BB21 has now been ruled out, significant regions still remain unobserved to the needed depth. Nonetheless, it is worth considering potential reasons why P9 was not found in the first 78% of parameter space surveyed. An obvious possibility, of course, is that Planet Nine does not exist. Such an explanation would require new explanations for multiple phenomena observed in the outer Solar System. Until such explanations are available, we continue to regard Planet Nine as the most likely hypothesis. Belyakov et al. (2022) explore the effects of different assumed colors, albedos, and radii for Planet Nine, and show that different choices of these parameters can change the amount of phase space covered by only of

order  $\sim 10\%$ . A potentially much larger effect would be a change in source region of the objects which become clustered by Planet Nine. In BB21, the assumption is made that the objects being observed are sourced from an early extended scattered disk. [Batygin & Brown \(2021\)](#) instead consider the effects of Planet Nine on objects pulled in from the inner Oort cloud and conclude that a similar clustering is observed for these objects but that the width of the cluster is broader. In BB21, the breadth of the cluster is directly related to the mass of Planet Nine and the broad cluster observed in the distant solar system is used to infer a lower mass, lower semimajor axis Planet Nine. If, instead, the observed breadth is caused by an inner Oort cloud source population for the clustered objects, the true Planet Nine could be more massive and more distant, making it potentially much fainter and harder to find. More work is required to explore this alternative version of the Planet Nine hypothesis.

## ACKNOWLEDGMENTS

The Pan-STARRS1 Surveys (PS1) and the PS1 public science archive have been made possible through contributions by the Institute for Astronomy, the University of Hawaii, the Pan-STARRS Project Office, the Max-Planck Society and its participating institutes, the Max Planck Institute for Astronomy, Heidelberg and the Max Planck Institute for Extraterrestrial Physics, Garching, The Johns Hopkins University, Durham University, the University of Edinburgh, the Queen's University Belfast, the Harvard-Smithsonian Center for Astrophysics, the Las Cumbres Observatory Global Telescope Network Incorporated, the National Central University of Taiwan, the Space Telescope Science Institute, the National Aeronautics and Space Administration under Grant No. NNX08AR22G issued through the Planetary Science Division of the NASA Science Mission Directorate, the National Science Foundation Grant No. AST-1238877, the University of Maryland, Eotvos Lorand University (ELTE), the Los Alamos National Laboratory, and the Gordon and Betty Moore Foundation.

## REFERENCES

- Babinet, M. 1848, *Comptes Rendus*, 27, 202
- Batygin, K., & Brown, M. E. 2016a, *AJ*, 151, 22, doi: [10.3847/0004-6256/151/2/22](https://doi.org/10.3847/0004-6256/151/2/22)
- . 2016b, *ApJL*, 833, L3, doi: [10.3847/2041-8205/833/1/L3](https://doi.org/10.3847/2041-8205/833/1/L3)
- . 2021, *ApJL*, 910, L20, doi: [10.3847/2041-8213/abee1f](https://doi.org/10.3847/2041-8213/abee1f)
- Belyakov, M., Bernardinelli, P. H., & Brown, M. E. 2022, *AJ*, 163, 216, doi: [10.3847/1538-3881/ac5c56](https://doi.org/10.3847/1538-3881/ac5c56)
- Bernardinelli, P. H., Bernstein, G. M., Sako, M., et al. 2022, *ApJS*, 258, 41, doi: [10.3847/1538-4365/ac3914](https://doi.org/10.3847/1538-4365/ac3914)
- Bernstein, G., & Khushalani, B. 2000, *AJ*, 120, 3323, doi: [10.1086/316868](https://doi.org/10.1086/316868)
- Brown, M. E., & Batygin, K. 2019, *AJ*, 157, 62, doi: [10.3847/1538-3881/aaf051](https://doi.org/10.3847/1538-3881/aaf051)
- . 2021, *AJ*, 162, 219, doi: [10.3847/1538-3881/ac2056](https://doi.org/10.3847/1538-3881/ac2056)
- . 2022, *AJ*, 163, 102, doi: [10.3847/1538-3881/ac32dd](https://doi.org/10.3847/1538-3881/ac32dd)
- Brown, M. E., Trujillo, C., & Rabinowitz, D. 2004, *ApJ*, 617, 645, doi: [10.1086/422095](https://doi.org/10.1086/422095)
- Chambers, K. C., Magnier, E. A., Metcalfe, N., et al. 2016, arXiv e-prints, arXiv:1612.05560. <https://arxiv.org/abs/1612.05560>
- Fienga, A., Di Ruscio, A., Bernus, L., et al. 2020, *A&A*, 640, A6, doi: [10.1051/0004-6361/202037919](https://doi.org/10.1051/0004-6361/202037919)
- Fortney, J. J., Marley, M. S., Laughlin, G., et al. 2016, *ApJL*, 824, L25, doi: [10.3847/2041-8205/824/2/L25](https://doi.org/10.3847/2041-8205/824/2/L25)

- Holman, M. J., Payne, M. J., Blankley, P., Janssen, R., & Kuindersma, S. 2018, *AJ*, 156, 135, doi: [10.3847/1538-3881/aad69a](https://doi.org/10.3847/1538-3881/aad69a)
- Madigan, A.-M., & McCourt, M. 2016, *MNRAS*, 457, L89, doi: [10.1093/mnrasl/slv203](https://doi.org/10.1093/mnrasl/slv203)
- Napier, K. J., Gerdes, D. W., Lin, H. W., et al. 2021, arXiv e-prints, arXiv:2102.05601. <https://arxiv.org/abs/2102.05601>
- Nesvorný, D., Bernardinelli, P., Vokrouhlický, D., & Batygin, K. 2023, *Icarus*, 406, 115738, doi: [10.1016/j.icarus.2023.115738](https://doi.org/10.1016/j.icarus.2023.115738)
- Scholtz, J., & Unwin, J. 2020, *PhRvL*, 125, 051103, doi: [10.1103/PhysRevLett.125.051103](https://doi.org/10.1103/PhysRevLett.125.051103)
- Sefilian, A. A., & Touma, J. R. 2019, *AJ*, 157, 59, doi: [10.3847/1538-3881/aaf0fc](https://doi.org/10.3847/1538-3881/aaf0fc)
- Shankman, C., Kavelaars, J. J., Bannister, M. T., et al. 2017, *AJ*, 154, 50, doi: [10.3847/1538-3881/aa7aed](https://doi.org/10.3847/1538-3881/aa7aed)
- Sivaram, C., Kenath, A., & Kiren, O. V. 2016, *Ap&SS*, 361, 230, doi: [10.1007/s10509-016-2815-z](https://doi.org/10.1007/s10509-016-2815-z)
- Standish, E. M. 1993, *AJ*, 105, 2000, doi: [10.1086/116575](https://doi.org/10.1086/116575)
- Tonry, J. L., Denneau, L., Flewelling, H., et al. 2018, *ApJ*, 867, 105, doi: [10.3847/1538-4357/aae386](https://doi.org/10.3847/1538-4357/aae386)
- Trujillo, C. A., & Sheppard, S. S. 2014, *Nature*, 507, 471, doi: [10.1038/nature13156](https://doi.org/10.1038/nature13156)
- Wu, Y., & Lithwick, Y. 2013, *ApJ*, 772, 74, doi: [10.1088/0004-637X/772/1/74](https://doi.org/10.1088/0004-637X/772/1/74)